

# Real time study of failure events in polymers

## Part I *Advanced methods for crack propagation studies of bulk polymer sections at the submicrometre level*

E. G. RIGHTOR, G. P. YOUNG, K. SEHANOBISH, J. C. CONBOY, C. P. BOSNYAK  
*Dow Chemical, Building B-1225, Freeport, TX 77541, USA*

Experimental methods have been developed so that *in situ* transmission electron microscope (TEM) tensile studies can be performed on bulk polymer sections, and failure processes observed; real time can be correlated with failure in bulk parts. Using specially designed support grids, polymer section geometry and *in situ* tensile procedures, the submicrometre failure response of polycarbonate–poly(ethylene terephthalate) phase morphology to crack propagation has been studied. This paper focuses on the design of the tensile grids, sections and procedures, which had to be devised for these studies. The techniques developed allow quantification of strain rates and crack velocities. TEM experiments performed showed that artefacts, such as vacuum or radiation damage, were not significant factors influencing the morphological response to crack propagation. A companion paper presents the failure processes found *in situ* and correlations with failure processes found in bulk tested parts.

### 1. Introduction

A key to commercial application of many polymer blends is an advanced understanding of the failure mechanisms that influence ultimate part performance. Historically, transmission electron microscopy (TEM) has been utilized to examine the response of various polymer phases to stress or strain, but the sample preparation methods used, such as post-mortem fixing of the crack [1], embedding [2], casting of thin films [3] or drawing of thin films from solution [4–9], do not allow real time study of the morphological response in an as-moulded specimen. With the last methods, the correspondence to real, bulk samples is also unknown. Real time scanning electron microscope (SEM) studies have provided some data on failure mechanisms [10], and acoustic emission has been correlated with failure events in an SEM [11]. However, this leaves little direct information about the sequence and mechanism of submicrometre failure initiation and propagation in bulk samples, where the effect of formulation and process variables on morphology is important.

The need to understand the response of phase morphology to stress in bulk polymers helped drive the development of methods for real time *in situ* TEM tensile studies. By preparing sections of bulk polymers on specially developed TEM tensile grids [12], submicrometre events can now be visualized, real time, without the above mentioned limitations [13]. As a first step towards advancing the fundamental description of these submicrometre events in polymer blends, methods were developed that would allow reproducible studies of crack propagation. A large

number of technical problems had to be resolved to allow studies of crack propagation in sections of bulk polymers in a way that would allow correlation to failure processes in bulk tested parts. In this paper these technical advances designed for studying the morphological response of polycarbonate–poly(ethylene terephthalate), PC–PET, to crack propagation are described. Part II [14] closely examines correlations between *in situ* failure events and failure events in bulk samples.

### 2. Experimental

The PC used for this work had a molecular weight,  $M_w$ , of 26 500 g mol<sup>-1</sup> and the commercially available PET had a  $M_w$  of 104 000 g mol<sup>-1</sup>. The experimental details for PC–PET 80/20 w/w mixing, injection moulding, etc., are given in Part II.

Sample blocks were trimmed to obtain sections one-third of the way from the skin to the core of the injection moulded sample. Sections were collected either parallel or perpendicular to the injection moulding direction depending on the experiment to be performed. To obtain the most reproducible crack propagation possible, a precrack was used at one edge of the sections as described below. The resulting blocks were microtomed at room temperature on a Reichert–Jung Ultracut E using a diamond knife. Sections were designed so that long sections with nearly parallel sides and tapered ends were obtained. Sections, 80–120 nm thick, were floated on water and picked up using a 1 × 2 mm single slotted grid which was used for exact positioning and alignment of sections in the viewing area. Unstained sections were

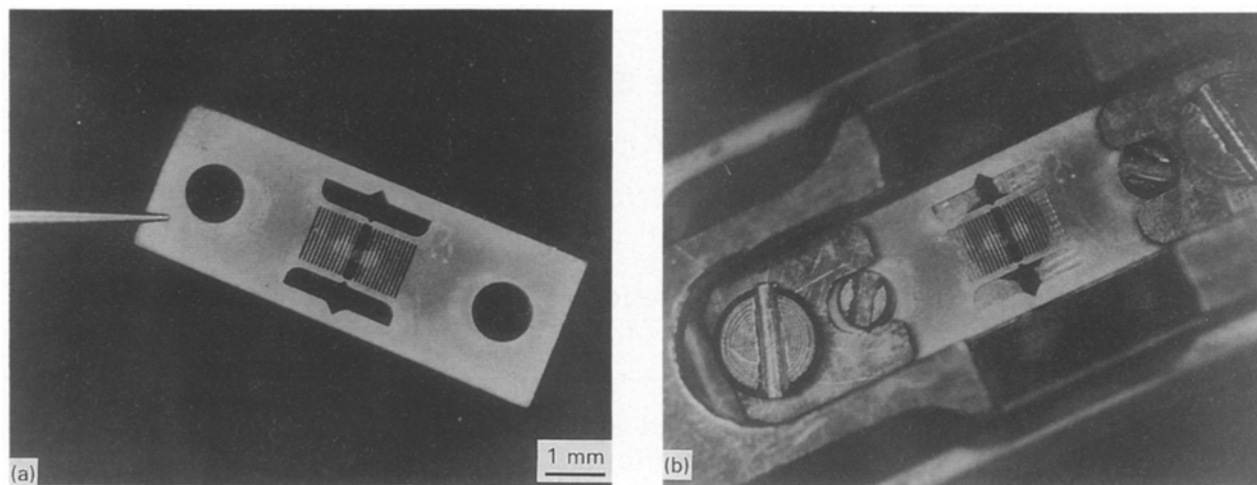


Figure 1 Optical micrographs of tensile grid with microtomed section stretching across centre opening (a) and (b) photo showing grid in tensile holder prior to stretching.

usually examined to avoid complications with chemical crosslinking. *In situ* TEM tensile experiments were performed in a JEOL 2000FX TEM using a JEOL tensile holder (model EM-SEH). An accelerating voltage of 200 kV was used for the majority of results in these papers. A Gatan model 673 camera was used for recording video images and to minimize radiation damage. TEM photographs were taken before and after the crack stopped. Photographs of slow moving sharp cracks were taken using fast TEM film (Kodak SO163) and short exposure times.

Sections were placed on specially designed copper support grids manufactured by PCM Products (Titusville, FL). The grids featured a large central area for viewing crack propagation. A number of closely spaced bars were placed on either side of the viewing area to hold the section and notches were carefully placed to aid controlled failure of the inner grid region. Failure of this inner grid region occurred first, and then the stress response in the sections was examined. Support grids were annealed at 700 °C in high vacuum (using a muffle furnace and quartz glassware) to make them ductile as mentioned earlier [7].

Measurements of crack geometry, crack radius of curvature, length, etc., were made from static TEM photos before pulling. The rate of pull was varied using a potentiometer to control the sample holder motor. The manufacturer's specifications state that the holder operates from  $0.05\text{--}0.65\ \mu\text{m s}^{-1}$  (when unloaded). The elongation rate was estimated by optical microscopy experiments (Wild M7A, reflected and transmitted light) where an annealed tensile grid was pulled outside the microscope at rates similar to those used during *in situ* TEM experiments. When a crack had progressed part way through the section, the displacement was decreased 0.05 mm and the holder was introduced into the TEM for photography.

### 3. Results and discussion

#### 3.1. Grid and section design

The emphasis of the current work on the response of phase morphology to crack propagation was different

than in earlier work [12], so the grid and section design were changed considerably. The design used provides a large area for viewing crack propagation, helps minimize anomalous edge effects associated with the grid bars, and provides a sample test geometry in line with the ratios of dimensions obtainable in bulk samples. This latter consideration is very important to enable correlations between *in situ* studies on PC-PET sections and bulk tensile tests followed by post-mortem TEM.

Experiments with and without sections on these grids showed that the reproducibility of failure of the copper grid itself was a concern. During tensile pulls, brittle behaviour of the copper resulted in catastrophic failure of the polymer section. It was impossible to follow such a fast crack at video rates, so this type of failure was avoided. A small notch on either side of the inner test area was added to give a well defined initiation site for failure, as shown in Fig. 1. The designed failure at the inner notch avoided substantial energy buildup in the copper and sudden catastrophic failure in the section when the copper grid failed. The outer grid would typically stay intact during the tensile pull.

To minimize complications in loading geometry, the typical trapezoidal section shape was avoided and instead sections with nearly parallel sides were prepared. Fig. 1 also illustrates the section shape for a section laying perpendicular to the viewing area (obscuring underlying portions of the copper bars). An oblong section shape was chosen to maximize the number of interactions between the section and support bars. This was important as the only "gripping" force on sections was the surface interactions with grid bars. The method of increasing the grid-specimen interactions through oblong sections proved adequate and straightforward.

To successfully orient undeformed sections parallel to the tensile axis and place them over the grid test area, sections were picked up using a slotted grid and positioned within the slotted grid using an eyelash brush. The section shape was tapered at the ends to make microtomy and alignment on the slotted and

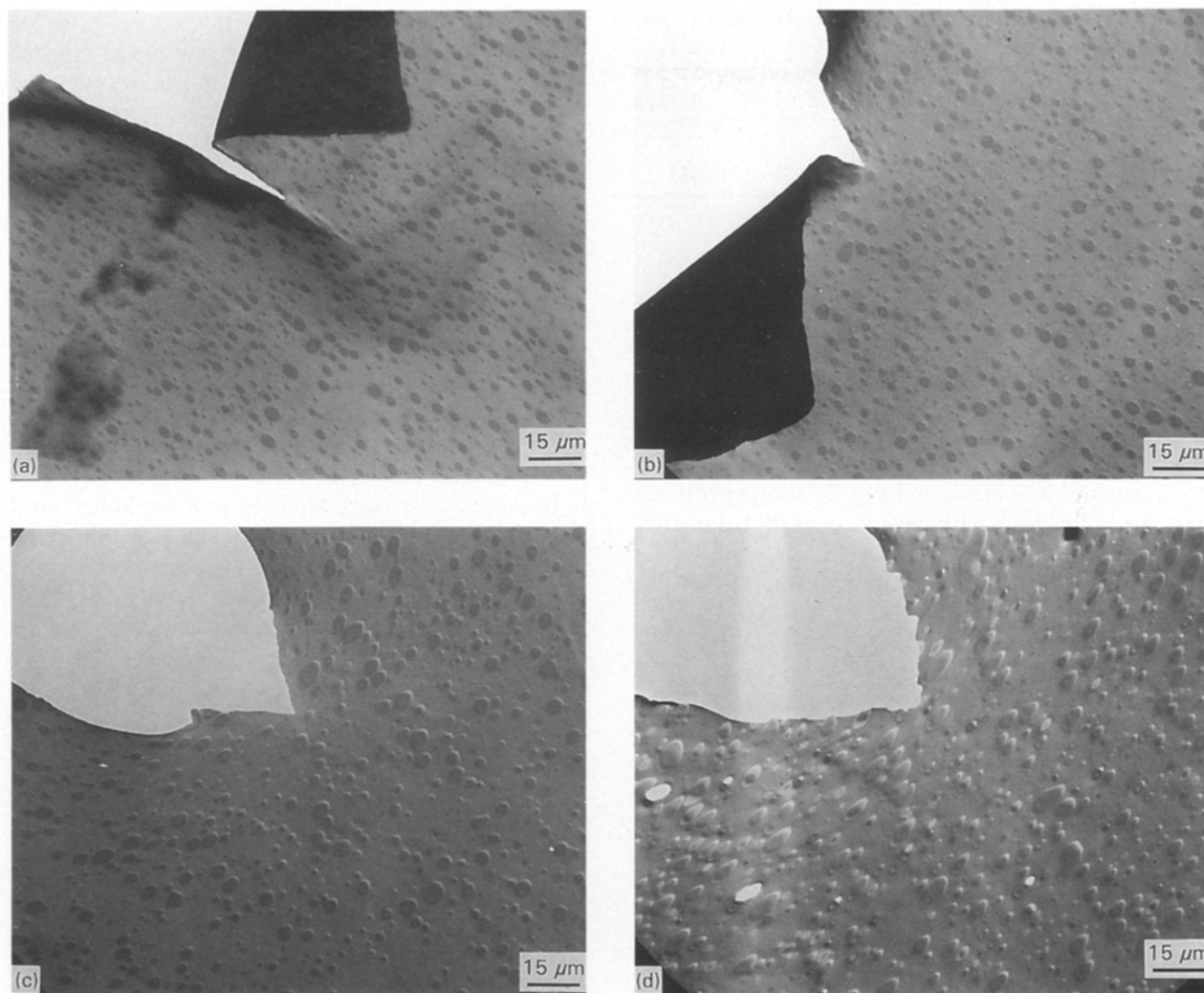


Figure 2 TEM micrographs showing (a) the prenotch at a section edge, (b) propagation of a sharp crack, (c) formation of a sharp crack from a blunted crack, and (d) propagation of a blunt crack with distortion of PET domains. The sections were cut perpendicular to flow giving discs of PET.

tensile grids easier. The section was then transferred to the tensile grids by placing the slotted grid on top of the tensile grid with the proper alignment. The work of Galey and Nilsson [15] was the basis for use of the slotted grid.

Preliminary experiments with PC-PET demonstrated that crack propagation could be more readily controlled if an initiation site was present at the edge of the polymer section. The method found to produce the sharpest, most reproducible precrack without additional sample damage was placement of a nick on one of the long edges of the pretrimmed sample block with a razor blade. This was accomplished by using the microtome to hold a piece of a razor blade, while the sample block was moved towards the blade using the precise lateral and forward controls on the microtome. The sample block was moved forward until a precrack  $\sim 20 \mu\text{m}$  deep was observed through the microtome binoculars. This value gave a notch length: section width of  $\sim 0.1 \mu\text{m}$ , which would be matched in bulk studies. The average length of the precrack in 11 representative experiments was  $16.5 \pm 4.6 \mu\text{m}$ , width at the sample edge  $6.9 \pm 4.1 \mu\text{m}$ , and radius of curvature  $0.13 \pm 0.03 \mu\text{m}$ . The measurements show that an exceptionally sharp (radius of curvature

similar to the razor blade used), fairly reproducible precrack was obtained using this method. During steady crack propagation the radius of curvature would rapidly go to  $< 0.2 \mu\text{m}$ , even for precracks that started out much broader.

Often the edge material on either side of the precrack would fold over forming flaps which would rest on top of the section. During tensile tests these flaps would cause reinforcement around the precrack resulting in buildup of stress (and eventually catastrophic failure). To minimize folding in the section area near the precrack, a technique was developed to invert the slotted grid containing the section on top of the tensile grid followed by drying of the section. A sharpened sliver of filter paper was used to carefully wick away excess water from the section. An antistatic gun was also used to help minimize flaps during transfer to the tensile grids. What was finally produced using these steps was a prenotched section oriented on the support grid which could be placed in the TEM tensile holder as shown in Fig. 1.

At higher magnification the sharpness of the prenotch made with the razor blade is clear, as shown in Fig. 2a for a section cut perpendicular to flow (PET

TABLE I Estimates of crack velocity in PC-PET sections from video tape

Relative crack speed	Crack velocity <sup>a</sup> ( $\mu\text{m s}^{-1}$ )
Slow crack	0.1–0.6
Fast crack	940–1450

<sup>a</sup> Assuming 1/30 s per video frame.

discs). This well defined initiation site allowed the experimentalist to know where to look for crack propagation during tensile pulls. The sequence of failure events during crack propagation could then be followed. Propagation of a slow, sharp crack is shown in Fig. 2b. Fig. 2c shows the formation of a sharp crack from a blunt crack and Fig. 2d shows propagation of a blunt crack with distortion of PET domains. This sequence of failure events could be recorded on video tape for a crack propagating through PC-PET.

### 3.2. Crack propagation and strain rates

The importance of crack propagation rate, explained in detail in [14], led to estimates of the rate of pull and crack growth in sections. The rate of pull measured at the inner grid or viewing area during optical microscopy experiments was divided by the section width to get the strain rate. The value found was  $3.9 \times 10^{-4} \text{ s}^{-1}$  (for a pull rate of 20% on the sample holder control). Grids made with different bar thicknesses, due to different degrees of chemical etching during manufacture, showed slightly different strain rates as expected. The velocity of crack propagation was also estimated for several experiments using the data from video tape, as shown in Table I.

### 3.3. *In situ* tensile procedures

After sections had been prepared on the support grids and dried briefly in a dessicator, they were introduced into the microscope vacuum. Care was taken to minimize radiation exposure to the sections during micro-

scope alignment, imaging and photography of the precrack, prior to tensile pulls. A video camera was used at low dose to preview the section and record real time failure. A high pull rate was used on the tensile device (100% on the potentiometer) to approach the point at which the grid started being drawn. The pull rate was reduced until the section was pulled tight, as indicated by elimination of any wrinkles, at which point the rate was decreased to 20%.

With sections cut perpendicular to flow (resulting in PET discs, as shown in [14]), this pull rate (of 10–20%) was typically maintained throughout steady crack propagation. For the sections cut parallel to flow with a prenotch placed parallel to flow, even 10% was usually too high to obtain steady crack propagation. When the crack was unstable and moved too fast to be recorded by video tape, the pull was halted until the crack came to a stop. Blunting of the crack tip was, in this case, typical, even when the pull was restarted immediately after the crack came to a stop. Upon further pulling, the blunt crack would progress for a while, until a sharp crack tip was formed at the front of the blunt crack. This sharp crack could be followed using low pull rates.

### 3.4. Examination of potential artefacts

To maximize the ability to correlate *in situ* TEM tensile studies with bulk tensile experiments, potential artefacts associated with the microscope vacuum, radiation damage and sample preparation (sectioning), were examined. Fig. 3 shows optical microscopy (OM) photos of a section being pulled at two different extensions. The strain in the copper holder and section is evident, as is the progressing crack in the section at 0.4 mm extension on the holder. Following extension to 0.42 mm the sample holder was introduced into the TEM, and photos were taken to document the response of PET domains to failure.

Fig. 4 shows representative TEM photos of polymer failure in sections that had been pulled outside of the TEM and monitored using an optical microscope. Typically, broader failure zones were seen in these

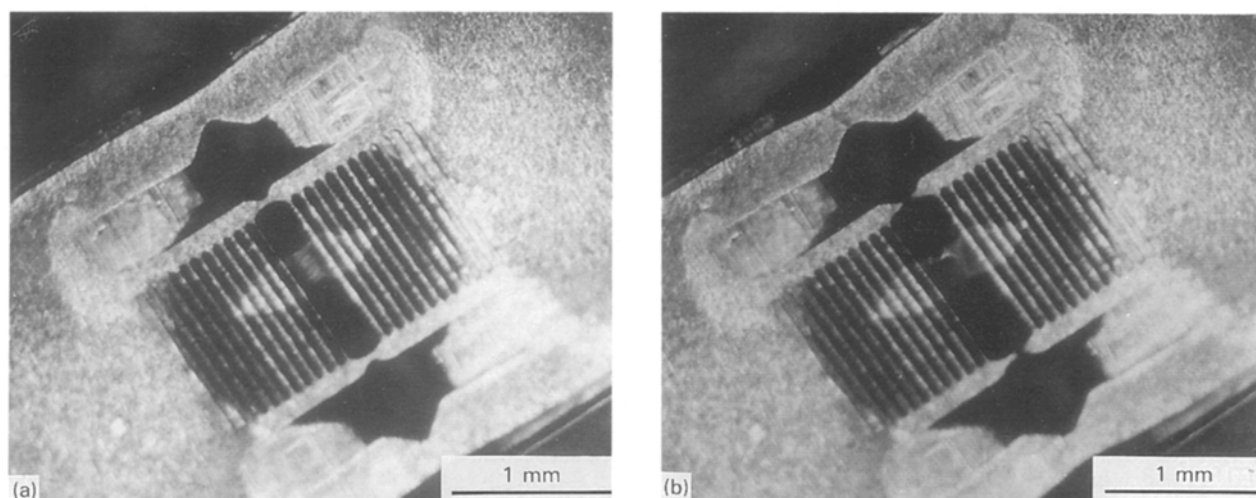


Figure 3 Optical micrographs showing sections being pulled in air under the microscope at (a) 0.3 mm and (b) 0.4 mm extension.

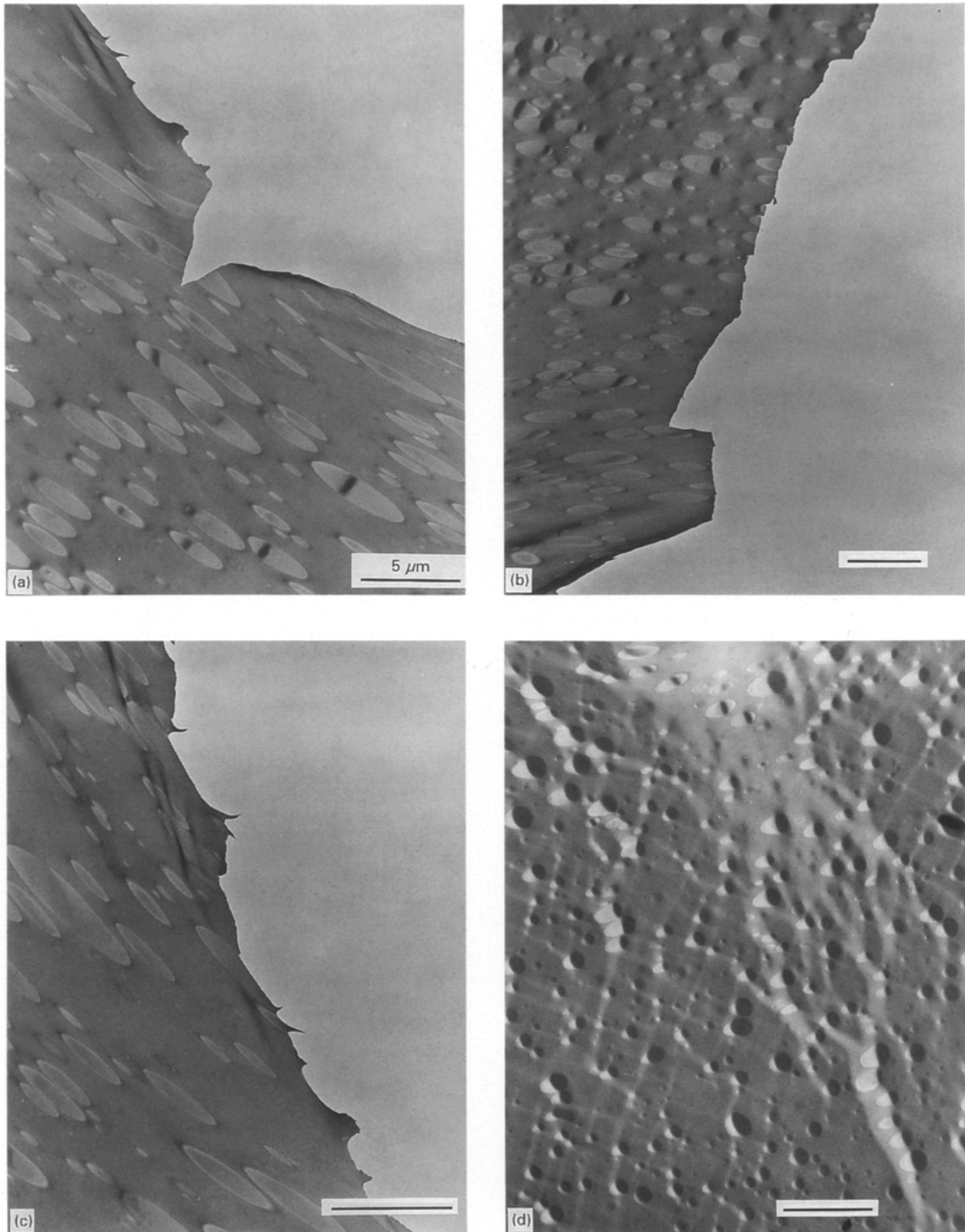


Figure 4 TEM micrographs showing PC-PET after pulling in air. The features shown are (a) a sharp crack propagating through moderately distorted PET domains, (b) crack path through smaller PET domains and around larger domains, (c) high distortion of PET 45° to the crack path, (d) local deformation bands in PC ahead of a blunt crack.

experiments, but the types of failure observed were very similar to those found in the TEM during *in situ* studies. Within the broad failure zone, significant distortion of the PET domains has occurred for the blunt crack that progressed up to the area shown in Fig. 4a (before a sharp crack started). This distortion of PET

domains was also seen by *in situ* TEM experiments for blunt cracks [14].

Evidence for deviation of the crack path for this broad crack around PET domains is also observed in the jagged crack surface. The PET in this case is drawn towards the crack centre and drawn remnants

of PET can be seen extending towards the crack surface, Fig. 4c. The formation of a very sharp crack at the blunt tip centre demonstrates movement of the crack directly through PET domains, Fig. 4a. These failure features are the same as those seen by *in situ* TEM experiments, i.e. PET bisection by crack, localized deformation bands, PET yielding, interfacial failure–crack deviation. However, in the OM experiments, a sharp slow brittle crack was not obtained. Several factors can be responsible for this difference, i.e. some electron beam damage, section thickness, flaps, desiccation, etc. It is known that polyesters absorb water with time, so plasticization of the PC–PET blends could occur (Goodyear commercial literature). The OM experiments were performed during the summer (e.g. humidity was not controlled) which may account for the slight differences observed in failure response.

It was also hypothesized that in cutting the polymer a molecular weight decrease may occur altering the failure observed in sections compared to bulk failure. To test this hypothesis, sections  $\sim 10\ \mu\text{m}$  thick were cut, and enough were collected ( $\sim 90$ ) to perform gel permeation chromatography (GPC). The molecular weight in the bulk and microtomed samples was similar. However, it is unknown if a molecular weight change occurs for TEM thickness sections.

#### 4. Conclusions

New *in situ* TEM techniques have been developed that allow analysis of failure processes with bulk polymer sections. Using specially designed copper support grids and section geometry, correlations between *in situ* and bulk failure processes can be examined. Estimates of pull rates, strain and crack velocity were also determined for comparison to bulk tests.

These methods have been tested using PC–PET, where the response of phase morphology to crack propagation at the submicrometre scale has been examined. The characteristic failure response to propagation of a sharp or blunt crack was found to be reproducible using these methods. The failure processes found using these methods correlate with failure in bulk polymer parts at a much larger scale, as

described in [14]. Tensile studies performed outside of the microscope showed behaviour similar to that observed during *in situ* TEM studies. Specifically, crack path deviation around PET domains, sharp cracks cutting through PET domains, PET distortion for blunt cracks were all found both during *in situ* and *ex situ* studies.

#### Acknowledgements

The authors acknowledge helpful technical discussions and joint work with R. C. Cieslinski at Dow Chemical, Midland. We also thank J. D. Allen for assistance with gel permeation chromatography on microtomed sections and E. T. Vreeland for dark room work.

#### References

1. R. P. KAMBOUR, *J. Polym. Sci.* **D7** (1973) 1.
2. H. J. SU, E. I. GARCIA-MEITIN, B. L. BURTON and C. C. GARRISON, *J. Polym. Sci., Part B Polym. Phys.* **29** (1991) 1623.
3. C. MAESTRINI and E. J. KRAMER, *Polymer* **32** (1991) 609.
4. D. C. YANG and E. L. THOMAS, *J. Mater. Sci.* **19** (1984) 2098.
5. B. D. LAUTERWASSER and E. J. KRAMER, *Phil. Mag. A* **39** (1979) 469.
6. L. L. BERGER and E. J. KRAMER, *J. Mater. Sci.* **22** (1987) 2739.
7. W. W. ADAMS, D. YANG and E. L. THOMAS, *ibid.* **21** (1986) 2239.
8. A. M. DONALD and E. J. KRAMER, *ibid.* **16** (1981) 2967.
9. G. MICHLER, *Colloid Polym. Sci.* **263** (1985) 462.
10. P. THEOCARIS, V. KYTOPOULOS and C. STASINAKIS, *J. Mater. Sci.* **24** (1989) 1121.
11. A. SIEGMANN and R. G. KANDER, *J. Mater. Sci. Lett.* **10** (1991) 619.
12. R. C. CIESLINSKI, *ibid.* **11** (1992) 813.
13. C. P. BOSNYAK, K. SEHANOBISH and E. G. RIGHTOR, *Amer. Chem. Soc. Polym. Prepr.* **33** (1992) 624.
14. E. G. RIGHTOR, K. SEHANOBISH, G. P. YOUNG, J. C. CONBOY, J. W. WINCHESTER and C. P. BOSNYAK, *J. Mater. Sci.* in press.
15. F. R. GALEY and S. E. G. NILSSON, *J. Ultrastruct. Res.* **14** (1966) 405.

Received 31 January  
and accepted 5 August 1991